Ideas and perspectives: How coupled is the vegetation to the boundary layer?

Martin G. De Kauwe[1,2], Belinda E. Medlyn[3], Jürgen Knauer[4], and Christopher A. Williams[5]

[1]ARC Centre of Excellence for Climate Extremes, University of New South Wales, Sydney, NSW 2052, Australia
[2]Department of Biological Science, Macquarie University, North Ryde NSW 2109 Australia
[3]Hawkesbury Institute for the Environment, Western Sydney University, Locked Bag 1797, Penrith NSW 2751 Australia
[4]Department of Biogeochemical Integration, Max Planck Institute for Biogeochemistry, 07745 Jena, Germany
[5]Graduate School of Geography, Clark University, 950 Main Street, Worcester, MA01602 USA

Correspondence to: Martin De Kauwe (mdekauwe@gmail.com)

Abstract. Understanding the sensitivity of transpiration to stomatal conductance is critical to simulating the water cycle. This sensitivity is a function of the degree of coupling between the vegetation and the atmosphere, and is commonly expressed by the decoupling factor. The degree of coupling assumed by models varies considerably and has previously been shown to be a major cause for model disagreement when simulating changes in transpiration in response to elevated CO_2. The degree of coupling also offers us insight into how different vegetation types control transpiration fluxes, fundamental to our understanding of land–atmosphere interactions. To explore this issue, we combined an extensive literature summary from 40 studies, with estimates of the decoupling coefficient estimated from FLUXNET data. We found some notable departures from values previously reported in single site studies. There was large variability in estimated decoupling coefficients (range = 0.05–0.51) for evergreen needleleaf forests. A result that was broadly supported by our literature review, but contrasts with the early literature which suggests evergreen needleleaf forests are generally well-coupled. Estimates from FLUXNET indicated that evergreen broadleaved forests were the most tightly coupled, differing from our literature review, which instead suggested it was evergreen needleleaf forests. We also found that the assumption that grasses would be strongly decoupled (due to vegetation stature) was only true for high precipitation sites. These results were robust to assumptions about aerodynamic conductance and energy balance closure. Thus, these data form a benchmarking metric against which to test model assumptions about coupling. Our results identify a clear need to improve the quantification of the processes involved in scaling from the leaf to the whole ecosystem. Progress could be made with targeted measurement campaigns at flux sites, as well as greater site characteristic information across the FLUXNET network.

1   Introduction

Predicting the response of transpiration to global change and the subsequent feedback to climate remains a major challenge for Earth system models (Zhu et al., 2017). Improving our understanding of how stomatal controls on transpiration vary between vegetation types is fundamental to simulating land–atmosphere interactions. Experimental evidence strongly indicates that stomatal conductance (G_s) is generally reduced in response to elevated CO_2 (Morison, 1985; Medlyn et al., 2001; Ainsworth

and Rogers, 2007), due to either a decrease in stomatal aperture with the reduced photosynthetic demand for CO_2 and/or a change in stomatal density (McElwain and Chaloner, 1995; Woodward and Kelly, 1995). In models, incorporating this leaf-level reduction in G_s commonly results in predictions of decreased transpiration and increased runoff at global scales (Gedney et al., 2006; Betts et al., 2007; Cao et al., 2010). However, the magnitude of this effect varies strongly among models, because the sensitivity of transpiration to a change in G_s depends on the assumption made about the strength of coupling of the vegetation to the surrounding boundary layer (McNaughton and Jarvis, 1983b; Jarvis and McNaughton, 1986; McNaughton and Jarvis, 1991; Jacobs and De Bruin, 1992). De Kauwe et al. (2013) identified differences in the degree of coupling to be a major cause of disagreement among 11 model predictions of transpiration in response to elevated CO_2 at two forest Free-Air CO_2 Enrichment (FACE) experiments in the USA. Consequently, resolving this discrepancy among models in their assumptions of vegetation-atmosphere coupling is key to reducing model uncertainty in future predictions of changes in transpiration.

The degree of coupling between vegetation and the atmosphere is commonly expressed by the decoupling factor (Ω; Jarvis and McNaughton, 1986). If the decoupling factor is high, transpiration is more strongly controlled by incoming radiation and less by changes in G_s. Low stature-canopies, and species with large leaves, are expected to be more decoupled (high Ω), than tall-stature canopies, and species with small leaves. This occurs, because: (i) small-stature canopies decrease the surface roughness, and hence the aerodynamic conductance; and (ii) large leaves decrease the leaf boundary layer conductance. Both act to diminish the rate of exchange between the vegetation surface and the atmosphere. Other characteristics of the vegetation, including, foliage clumping, leaf shape, canopy density and the vertical canopy distribution, will also alter the coupling. Values given in the literature for coniferous forests are typically low, $\Omega = {\sim}0.1\text{-}0.2$ (Whitehead et al., 1984; Jarvis, 1985; Lee and Black, 1993; Meinzer et al., 1993). Values are typically higher for deciduous broadleaved: $\Omega = 0.2\text{-}0.4$ (Magnani et al., 1998; Wullschleger et al., 2000), evergreen broadleaved species: $\Omega = 0.4\text{-}0.9$ (Meinzer et al., 1997; Wullschleger et al., 1998), grasses: $\Omega = 0.8$ (McNaughton and Jarvis, 1983a), and crops: $\Omega = 0.2\text{-}0.9$ (Black et al., 1970; Brown, 1976; Meinzer et al., 1993; Mielke et al., 1999). These literature estimates of the degree of coupling are wide and thus, do not offer a clear constraint to models. Furthermore, methods to estimate Ω often differ across studies, which complicates interpretations about variation across plant functional types. Single studies, that have employed a consistent method to estimate Ω across multiple species are rare (e.g. Stoy et al., 2006).

There has been considerable recent effort to develop better global datasets of stomatal behaviour for use by the modelling community (Lin et al., 2015; Miner et al., 2017). However, constraining the coupling between stomatal conductance and transpiration is equally important. For example, De Kauwe et al. (2015) demonstrated modest changes in transpiration when using the Lin et al. (2015) dataset to constrain the parameterisation of G_s in the Community Atmosphere Biosphere Land Exchange (CABLE) land surface model. The CABLE model assumes a relatively weak level of coupling (De Kauwe et al., 2013). It is likely that models that assume stronger coupling (e.g. the Joint UK Land Environment Simulator, JULES; Best et al., 2011) would obtain different results.

To shed new light on this important question of vegetation-atmosphere coupling, we used eddy-covariance data from FLUXNET to estimate the Ω coefficient for different plant functional types (PFTs). We aimed to: (i) examine if decoupling

coefficients estimated from FLUXNET were consistent with literature values; and (ii) develop a benchmark metric against which to test model assumptions about coupling.

2 Materials and Methods

2.1 Flux Data

Half-hourly eddy covariance measurements of the exchange of carbon dioxide, energy and water vapour were obtained from the FLUXNET "La Thuile" Free and Fair dataset (http://www.fluxdata.org). We estimated the degree of decoupling (Jarvis and McNaughton, 1986) as:

$$\Omega = \frac{1 + \epsilon}{1 + \epsilon + \frac{G_a}{G_s}} \tag{1}$$

where $\epsilon = s\,/\,\gamma$, s is the slope of the saturation vapour pressure curve at air temperature (Pa K^{-1}), γ is the psychrometric constant (Pa K^{-1}) and λ is the latent heat of water vapour (J mol^{-1}).

We estimated values of G_s by inverting the Penman-Monteith equation using measured latent heat (LE) flux for all datasets where the net radiation (R_n; W m^{-2}) and the frictional velocity (u_*; m s^{-1}) were available:

$$G_s = \frac{G_a \gamma \lambda E}{s(R_n - G) - (s + \gamma)\lambda E + G_a M_a c_p D} \tag{2}$$

where G_a (mol m^{-2} s^{-1}) is the canopy aerodynamic conductance, E (mol m^{-2} s^{-1}) is the canopy transpiration, γ is the psychrometric constant (Pa K^{-1}), D (Pa) is the vapour pressure deficit, G (W m^{-2}) is the soil heat flux, M_a (kg mol^{-1}) is molar mass of air, c_p is the heat capacity of air (J kg^{-1} K^{-1}). At sites where values of G were not available, G was set to zero.

G_a was calculated following Thom (1975):

$$G_a = \frac{c}{\frac{u}{u_*^2} + 6.2 u_*^{-\frac{2}{3}}} \tag{3}$$

where c = P / ($R_{gas}\,T_k$) is a conversion factor from units of m s^{-1} to mol m^{-2} s^{-1}, P is atmospheric pressure (Pa), R_{gas} is the gas constant (J mol^{-1} K^{-1}), T_k is the air temperature in Kelvin, and u (m s^{-1}) is the wind speed.

In our analysis we derived the average (three most productive months) decoupling coefficient, as the focus of our manuscript was on the spatial variability in coupling across FLUXNET. This is likely to be a metric that can most readily be exploited to assess existing coupling assumptions in models. Future analysis may wish to explore the temporal variability in this metric.

The approach we have taken (similar to Jarvis and McNaughton, 1986) ignores differences between canopy and air temperature (radiative coupling) within the canopy (see Martin, 1989). However, correcting for the longwave radiative conductance

(G_r) most impacts vegetation with the weakest control on transpiration the most and as a result, this assumption has little impact on the degree of coupling range for forest species, but may be a factor for other species.

Flux data were first screened as follows: (i) data flagged as "good" (quality control flag "fqcOK" = 1; Williams et al., 2012); (ii) data from the three most productive months, to account for the different timing of summer in the Northern and Southern hemispheres; (iii) daylight hours between 8 am and 4 pm, to account for periods when the vegetation is photosynthesising; (iv) half-hours with precipitation, and the subsequent 48 half-hours, were excluded to minimise the influence of soil evaporation (Law et al., 2002; Groenendijk et al., 2011; Dekker et al., 2016); and (v) data with a $u_* < 0.25$ were excluded to avoid conditions of low turbulence (Sánchez et al., 2010). We also excluded sites classified as mixed-forest, permanent wetlands or those where the PFT was unclassified.

Pressure was estimated using the hypsometric equation based on site elevation data. Where site elevation information was missing, values were gap-filled using the 30-arc second (~1 km) global digital elevation model GTOPO30 data from the United States Geological Survey (USGS). After filtering, 164 sites and 592 site-years remained.

We also tested the sensitivity of estimated values to: (i) errors in G_a; and (ii) errors due to a lack of energy balance closure. First, we increased/decreased estimated values of G_a by 30% to examine the sensitivity of G_s values inverted from the Penman-Monteith equation. Secondly, following recommendations by Wohlfahrt et al. (2009), we tested the sensitivity of our results to energy balance closure, by correcting the Bowen-ratio (each half-hourly LE and H flux) based on the available energy (Rn–G) on a longer time scale (three most productive months).

We also replicated our analysis using eddy covariance data taken from the FLUXNET2015 dataset (http://fluxnet.fluxdata.org/data/fluxnet2015-dataset). Figure A1 is a replicate of Fig. 1 and shows the patterns we derived are robust across flux releases.

2.2 Results

We summarised previously reported estimates of the decoupling coefficient from 40 studies, covering 57 PFTs, in Tables 1 and A2. Broadly speaking, estimated decoupling coefficients from FLUXNET (Fig. 1) differed among PFTs in line with literature values (Tables 1 and A2) and in line with expectations related to vegetation roughness and/or stature. Evergreen needleleaf forests (ENF), which have small leaves, were in general tightly coupled (low Ω), while deciduous broadleaved forests, tropical rain forest (large leaves), grasses and crops (small stature), had a lower degree of coupling (higher Ω). However, there were some notable departures from expectations. Estimates derived from FLUXNET indicated that evergreen broadleaf forests were the most coupled PFT (mean $\Omega = 0.21$) as opposed to the literature review, which suggested ENF PFTs were the most coupled (mean $\Omega = 0.19$). The FLUXNET data also indicated unexpectedly wide ranges for Ω within PFTs. For grasses, Ω ranged from 0.02–0.81; the number of low values was particular suprising, given the expectation that shorter stature vegetation would be more decoupled.

The wide range in estimagted values for ENF sites was also striking; Ω extended from 0.05 to 0.51. To attempt to better understand this range, we first separated ENF sites into: (a) sites with a low inter-annual coefficient of variation (20%), indicating consistent year-to-year estimates of the degree of coupling; (ii) sites with a coefficient of variation > 20%, indicating sites

with year-to-year variability in coupling; and (iii) sites with only two years of data. This separation was intended to rule out sampling issues. Figure 2 shows that the variability in the estimated decoupling coefficient cannot be explained by sampling bias, with significant site-to-site variability, irrespective of the inter-annual variability.

We then probed these results for relationships with site variables, by testing to see if: (i) sites with higher precipitation (in the three most productive months) were more decoupled, where precipitation was assumed to be a proxy for leaf area index (LAI)/productivity; or (ii) windy sites were more coupled. For grasses we found a significant relationship between the degree of coupling and precipitation (Fig. 3). The data suggest that for sites that are likely to be more open grasslands (i.e. sites with a low precipitation) the vegetation is very coupled to the atmosphere, with a high level of stomatal control. This relationship between the degree of coupling and precipitation (r=0.46) explains the high variability in estimated decoupling coefficients for grasses shown in Fig. 1. The prediction that grasses would be weakly coupled due to small vegetation stature only holds true at sites with high 3-month precipitation, which are presumably sites with high LAI. We also found a significant relationship for ENF sites (r=0.40), and deciduous broadleaved forests (r=0.64) suggesting that the degree of coupling declined with canopy density. We also found evidence of a weak negative relationship (r=−0.21) between wind speed and the degree of coupling for forest sites, i.e. windier sites tended to be more coupled (Fig 4). For non-forest PFTs, we did not find a significant relationship between wind speed and coupling.

Finally, we examined sensitivity of our results to potential errors. We tested whether our results were sensitive to different estimates of G_a and whether our estimates of G_s were sensitive to energy imbalance. We found that the broad pattern of our results in Fig. 1 was insensitive to errors in G_a. Increasing or decreasing G_a by 30%, led to the median decoupling coefficient decreasing or increasing by roughly 0.05 for evergreen broadleaf forest (EBF) sites for example. However, we did find that our results were sensitive to a correction for the lack of energy balance closure. Figure A2 shows that attempting to correct for a lack of closure leads to sites becoming less coupled, but does not shift the between-PFT differences in the degree of coupling. The largest changes were for C3 crops (Ω changed from ~0.44 to ~0.6) and deciduous broadleaved forests (Ω changed from ~0.31 to ~0.41).

2.3 Discussion

Correctly characterising the sensitivity of transpiration to G_s is critical for simulating the water cycle, particularly for future projections of the terrestrial biosphere where it is widely expected that G_s will decrease in response to increasing atmospheric CO_2. The parameterisation of this crucial link between leaf– and canopy–scale water fluxes has been largely ignored in model studies addressing the impact of elevated CO_2 (Betts et al., 2007; Cao et al., 2010; Zhu et al., 2017). Resulting projections of changes in transpiration and associated fluxes (e.g. runoff, precipitation) are likely to be model-specific, with large uncertainty among models (De Kauwe et al., 2013). Model studies rarely provide information about the degree of coupling assumed within the model. The range of assumptions commonly incorporated in models include: (i) coupling is a function of roughness length (determined by vegetation height), e.g. JULES; (ii) coupling is a function of leaf size, e.g. CLM (the Community Land Model; Oleson et al., 2013); (iii) coupling is affected by within canopy turbulence, e.g. CABLE (Raupach et al., 1997; Kowalczyk et al., 2006); (iv) some combination of all three, e.g. CABLE/CLM; (v) coupling is not sensitive to wind speed (i.e. wind speed

is fixed to 5 m s^{-1}), e.g. SDGVM (Sheffield Dynamic Global Vegetation Model; Woodward et al., 1995); or (vi) models that use an alternative to the Penman-Monteith equation, e.g. LPJ (Lund-Potsdam-Jena family of models; Sitch et al., 2003). This family of models use an empirically calibrated hyperbolic function of canopy conductance (Huntingford and Monteith, 1998) and the implied level of coupling depends on how this function is parameterised.

5   Understandably, the pioneering work of Jarvis and McNaughton (1986) is widely cited when issues of coupling are discussed in the literature. However, many of the earlier estimates of coupling they summarised were taken from single sites and thus does not necessarily reflect the diversity of global vegetation. In this study we have summarised 40 literature studies, covering 57 PFT, in combination with estimates of the decoupling coefficient from 164 sites and 592 site-years from FLUXNET. Our literature summary (Tables 1 and A2) highlights the diversity of approaches used to determine Ω. In contrast, we have applied a consistent methodology across all the 164 FLUXNET sites. For forest PFTs, our results point to a weaker level of coupling than is often assumed. Notably, ENF species were found to be less coupled (mean $\Omega = 0.21$; range $= 0.05$–0.51) across FLUXNET than summarised in Jarvis and McNaughton (1986) ($\Omega = 0.1$). Our estimate derived from FLUXNET was supported by our wider literature summary (n=13). We found that the often assumed low degree of coupling for grasses is likely to only be true for high precipitation (and presumably high LAI) sites; low precipitation sites were strongly coupled. A further plausible explanation is that these drier sites are limited by available soil moisture, with lower G_s resulting in a high degree of coupling. We could not easily explain the coupling values estimated for evergreen broadleaf forests, which were estimated to be more coupled than evergreen needleleaf forests; a break from theoretical understanding developed from vegetation roughness and/or stature. Finally, grouping the data by PFTs also highlighted marked within-PFT variation in the degree of coupling.

       As land models move towards more realistic representations of the variability of stomatal conductance (De Kauwe et al., 2015), informed by leaf-level syntheses (Lin et al., 2015; Miner et al., 2017), it is also important that they accurately simulate the coupling between vegetation and the atmosphere. Without this focus, any efforts to improve the realism at the leaf-scale will not be reflected in improvements in simulated transpiration at the canopy scale.

2.3.1   Caveats

One criticism of the approach taken here is that we have assumed a big-leaf approximation to estimate vegetation the degree of coupling (see Raupach and Finnigan, 1988). It is of course likely that variation within a canopy in terms of micro-climate (i.e. vapour pressure deficit, irradiance, temperature), as well as how stomata respond, may invalidate this approach. Use of a big-leaf approximation could be a possible explanation for the surprisingly high level of coupling found in evergreen broadleaf forests, although it would appear unlikely given the weaker level of coupling found for deciduous broadleaved and tropical rainforest species.

30   We found high variation in the estimated coupling factor both across sites and within sites. Two assumptions we make with respect to the flux data could explain this variation. Firstly, we excluded data following rainfall (48 hours) (Law et al., 2002; Groenendijk et al., 2011; Dekker et al., 2016) to minimise the effects of soil evaporation. Clearly, if soil evaporation is still a component of the LE flux after this point it would introduce error to our estimates. This assumption may also vary with PFT. Secondly, flux towers commonly do not close the energy balance (Foken, 2008; Wilson et al., 2002). Our use of the

inverted Penman-Monteith equation implies that we are attributing any errors due to energy imbalance to the sensible heat flux. Additionally, where data on the soil heat flux were missing, we assumed there was no storage. Correcting for these issues is not straightforward as it requires determining which flux is the source of the error (see Wohlfahrt et al., 2009, for a detailed discussion). We followed recommendations by Wohlfahrt et al. (2009) and tested the sensitivity of our results to energy balance closure, by correcting the Bowen-ratio based on the available energy (Rn–G). Whilst we did find some sensitivity in our results (particularly for C3 crops and deciduous broadleaved forests), it did not change the ordering of coupling factors between PFTs, or explain the unexpected high level of coupling for EBF sites.

Finally, we estimated the canopy aerodynamic conductance (G_a) using an empirical equation following Thom (1975). Knauer et al. (2017) tested the impact on different methods of estimating G_a from flux data on estimates of the stomatal slope parameter (the sensitivity of stomatal conductance to assimilation). They found that correcting G_a for atmospheric instabilities only led to small increases in estimates of G_a during daytime growing conditions. They also found that a more physically-based representation of G_a (Su et al., 2001), led to lower estimate of G_a at two EBF flux sites, and higher estimates of G_a at another EBF and a deciduous broadleaved site. We tested the sensitivity of our results to a change in G_a of the order shown by Knauer et al. (2017) and found the patterns in coupling to be robust across PFTs.

2.3.2 Route forward

Estimates of coupling from ecosystem scale flux data are directly relevant for models. We previously speculated (De Kauwe et al., 2013) that discrepancies among models in coupling might be resolved by examining eddy covariance data. The range in coupling factors we have estimated from the FLUXNET data provides an overall constraint on the degree of coupling that should be assumed in models, as well as an indication of the appropriate degree of variability in coupling across PFTs and rainfall regimes. The next steps involve determining what models currently assume about the degree of coupling and then to determine how flux-derived estimates of coupling would change model predictions.

In this study we examined the long-term average coupling factor. It may also be instructive to consider how estimated coupling factors change across the course of a day or within a season. However, it is likely that such an approach may be more sensitive to noise in the fluxes as well as events such as drought.

Our results also identify a clear need to better understand leaf-to-atmosphere coupling. We need to better understand why coupling factors vary within PFTs. There are a number of plausible explanations, such as drought, diversity of vegetation within a flux footprint, data issues, and it is likely that more detailed site-specific insight will be required to move forward. To assist in better understanding patterns, we will need greater detail in terms of ancillary data from FLUXNET sites. We attempted to probe our results with respect to canopy height and LAI, but for many sites this information was not available. Other potentially useful information would include leaf size, stem density and crown length, and whether canopy height is static or increasing. These data would facilitate more sophisticated approaches to be explored, for example stability corrections and/or estimates of G_a based on leaf size (Su et al., 2001). A more fundamental process understanding will require targeted G_s measurements throughout the canopy, alongside corresponding sap flux measurements in forests and chamber measurements in grasslands. Recently, Medlyn et al. (2017) compared estimates of plant water-use efficiency derived from leaf gas exchange data and eddy

flux data for eight sites where these measurements were acquired at the same point in time. They found similarities for DBF and TRF PFTs, but differences for EBF and ENF PFTs. The authors were unable to explain these scaling discrepancies. Further targeted measurements campaigns at flux sites could lead to new knowledge, which would advance our understanding of the processes involved in scaling from the leaf to the canopy.

5 *Code availability.* All code is freely available from: https://github.com/mdekauwe/flux_decoupling

Data availability. All Eddy covariance data are available from: http://fluxnet.fluxdata.org/data/la-thuile-dataset/

Competing interests. The authors declare no competing financial interests.

Acknowledgements. M.G. De Kauwe was supported by an Australian Research Council Linkage grant LP140100232. This work used eddy covariance data acquired by the FLUXNET community and in particular by the following networks: AmeriFlux (U.S. Department of Energy, Biological and Environmental Research, Terrestrial Carbon Program (DE–FG02–04ER63917 and DE–FG02– 04ER63911)), AfriFlux, AsiaFlux, CarboAfrica, CarboEuropeIP, CarboItaly, CarboMont, ChinaFlux, Fluxnet–Canada (supported by CFCAS, NSERC, BIOCAP, Environment Canada, and NRCan), GreenGrass, KoFlux, LBA, NECC, OzFlux, TCOS–Siberia, USCCC. We acknowledge the financial support to the eddy covariance data harmonization provided by CarboEuropeIP, FAO–GTOS–TCO, iLEAPS, Max Planck Institute for Biogeochemistry, National Science Foundation, University of Tuscia, Université Laval and Environment Canada and US Department of Energy and the database development and technical support from Berkeley Water Center, Lawrence Berkeley National Laboratory, Microsoft Research eScience, Oak Ridge National Laboratory, University of California, University of Virginia.

References

Ainsworth, E. and Rogers, A.: The response of photosynthesis and stomatal conductance to rising [CO_2]: mechanisms and environmental interactions, Plant, Cell and Environment, 30, 258–270, doi:10.1111/j.1365-3040.2007.01641.x, 2007.

Aires, L., Pio, C., and Pereira, J.: The effect of drought on energy and water vapour exchange above a mediterranean C3/C4 grassland in Southern Portugal, Agricultural and Forest Meteorology, 148, 565–579, 2008.

Best, M. J., Pryor, M., Clark, D. B., Rooney, G. G., Essery, R. L. H., Ménard, C. B., Edwards, J. M., Hendry, M. A., Porson, A., Gedney, N., Mercado, L. M., Sitch, S., Blyth, E., Boucher, O., Cox, P. M., Grimmond, C. S. B., and Harding, R. J.: The Joint UK Land Environment Simulator (JULES), model description – Part 1: Energy and water fluxes, Geoscientific Model Discussions, 4, 677–699, 2011.

Betts, R., Boucher, O., Collins, M., Cox, P., Falloon, P., Gedney, N., Hemming, D., Huntingford, C., Jones, C., Sexton, D., and Webb, M. J.: Projected increase in continental runoff due to plant responses to increasing carbon dioxide, Nature, 448, 1037–1041, 2007.

Black, T. A., Tanner, C., and Gardner, W.: Evapotranspiration from a snap bean crop, Agronomy Journal, 62, 66–69, 1970.

Bladon, K. D., Silins, U., Landhäusser, S. M., and Lieffers, V. J.: Differential transpiration by three boreal tree species in response to increased evaporative demand after variable retention harvesting, Agricultural and forest meteorology, 138, 104–119, 2006.

Bracho, R., Powell, T. L., Dore, S., Li, J., Hinkle, C. R., and Drake, B. G.: Environmental and biological controls on water and energy exchange in Florida scrub oak and pine flatwoods ecosystems, Journal of Geophysical Research: Biogeosciences, 113, 2008.

Brown, K. W.: Vegetation and the Atmosphere, chap. Sugar beet and potatoes, Academic Press, London, 1976.

Cao, L., Bala, G., Caldeira, K., Nemani, R., and Ban-Weiss, G.: Importance of carbon dioxide physiological forcing to future climate change, PNAS, 107, 9513–9518, doi:10.1073/pnas.0913000107, 2010.

Daudet, F., Le Roux, X., Sinoquet, H., and Adam, B.: Wind speed and leaf boundary layer conductance variation within tree crown: consequences on leaf-to-atmosphere coupling and tree functions, Agricultural and Forest Meteorology, 97, 171–185, 1999.

De Kauwe, M. G., Medlyn, B. E., Zaehle, S., Walker, A. P., Dietze, M. C., Hickler, T., Jain, A. K., Luo, Y., Parton, W. J., Prentice, I. C., Smith, B., Thornton, P. E., Wang, S., Wang, Y.-P., Wårlind, D., Weng, E., Crous, K. Y., Ellsworth, D. S., Hanson, P. J., Seok Kim, H., Warren, J. M., Oren, R., and Norby, R. J.: Forest water use and water use efficiency at elevated CO_2: a model-data intercomparison at two contrasting temperate forest FACE sites, Global Change Biology, 19, 1759–1779, doi:10.1111/gcb.12164, 2013.

De Kauwe, M. G., Kala, J., Lin, Y.-S., Pitman, A. J., Medlyn, B. E., Duursma, R. A., Abramowitz, G., Wang, Y.-P., and Miralles, D. G.: A test of an optimal stomatal conductance scheme within the CABLE land surface model, Geoscientific Model Development, 8, 431–452, doi:10.5194/gmd-8-431-2015, 2015.

Dekker, S. C., Groenendijk, M., Booth, B. B. B., Huntingford, C., and Cox, P. M.: Spatial and temporal variations in plant water-use efficiency inferred from tree-ring, eddy covariance and atmospheric observations, Earth System Dynamics, 7, 525–533, 2016.

Foken, T.: The energy balance closure problem: an overview, Ecological Applications, 18, 1351–1367, 2008.

Gaofeng, Z., Ling, L., Yonghong, S., Xufeng, W., Xia, C., Jinzhu, M., Jianhua, H., Kun, Z., and Changbin, L.: Energy flux partitioning and evapotranspiration in a sub-alpine spruce forest ecosystem, Hydrological processes, 28, 5093–5104, 2014.

Gedney, N., Cox, P., Betts, R., Boucher, O., Huntingford, C., and Stott, P.: Detection of a direct carbon dioxide effect in continental river runoff records, Nature, 439, 835–838, doi:10.1038/nature04504, 2006.

Goldberg, V. and Bernhofer, C.: Testing different decoupling coefficients with measurements and models of contrasting canopies and soil water conditions, in: Annales geophysicae: atmospheres, hydrospheres and space sciences, vol. 26, p. 1977, 2008.

Granier, A. and Bréda, N.: Modelling canopy conductance and stand transpiration of an oak forest from sap flow measurements, in: Annales des Sciences Forestieres, vol. 53, pp. 537–546, EDP Sciences, 1996.

Groenendijk, M., Dolman, A., van der Molen, M., Leuning, R., Arneth, A., Delpierre, N., Gash, J., Lindroth, A., Richardson, A., Verbeeck, H., et al.: Assessing parameter variability in a photosynthesis model within and between plant functional types using global Fluxnet eddy covariance data, Agricultural and Forest Meteorology, 151, 22–38, 2011.

Haijun, L., Cohen, S., Lemcoff, J. H., Israeli, Y., and Tanny, J.: Sap flow, canopy conductance and microclimate in a banana screenhouse, Agricultural and Forest Meteorology, 201, 165–175, 2015.

Hao, Y., Wang, Y., Huang, X., Cui, X., Zhou, X., Wang, S., Niu, H., and Jiang, G.: Seasonal and interannual variation in water vapor and energy exchange over a typical steppe in Inner Mongolia, China, Agricultural and Forest Meteorology, 146, 57–69, 2007.

Herbst, M.: Stomatal behaviour in a beech canopy: an analysis of Bowen ratio measurements compared with porometer data, Plant, Cell & Environment, 18, 1010–1018, 1995.

Hinckley, T., Brooks, J., Čermák, J., Ceulemans, R., Kučera, J., Meinzer, F., and Roberts, D.: Water flux in a hybrid poplar stand, Tree Physiology, 14, 1005–1018, 1994.

Huntingford, C. and Monteith, J.: The behaviour of a mixed-layer model of the convective boundary layer coupled to a big leaf model of surface energy partitioning, Boundary-Layer Meteorology, 88, 87–101, 1998.

Iida, S., Ohta, T., Matsumoto, K., Nakai, T., Kuwada, T., Kononov, A. V., Maximov, T. C., van der Molen, M. K., Dolman, H., Tanaka, H., et al.: Evapotranspiration from understory vegetation in an eastern Siberian boreal larch forest, Agricultural and Forest Meteorology, 149, 1129–1139, 2009.

Jacobs, C. and De Bruin, H.: The sensitivity of regional transpiration to land-surface characteristics: significance of feedback, Journal of Climate, 5, 683–698, 1992.

Jarvis, P.: The interpretation of the variations in leaf water potential and stomatal conductance found in canopies in the field, Philosophical Transactions of the Royal Society of London. Series B, Biological Sciences, 273, 593–610, 1976.

Jarvis, P. and McNaughton, K.: Stomatal control of transpiration: Scaling up from leaf to region, Advances in Ecological Research, 15, 1–49, 1986.

Jarvis, P. G.: Attributes of Trees as Crop Plants, chap. Transpiration and assimilation of tree and agricultural crops: the omega factor, pp. 460–480, Institute of Terrestrial Ecology, 1985.

Jassal, R. S., Black, T. A., Spittlehouse, D. L., Brümmer, C., and Nesic, Z.: Evapotranspiration and water use efficiency in different-aged Pacific Northwest Douglas-fir stands, Agricultural and forest meteorology, 149, 1168–1178, 2009.

Knauer, J., Zaehle, S., Medlyn, B., Reichstein, M., Williams, C. A., Migliavacca, M., De Kauwe, M. G., Werner, C., Keite, C., Kolari, P., Limousin, J.-M., and Linderson, M.-J.: Towards physiologically meaningful water-use efficiency estimates from eddy covariance data, Global Change Biology, in press, 2017.

Köstner, B., Schulze, E.-D., Kelliher, F., Hollinger, D., Byers, J., Hunt, J., McSeveny, T., Meserth, R., and Weir, P.: Transpiration and canopy conductance in a pristine broad-leaved forest of Nothofagus: an analysis of xylem sap flow and eddy correlation measurements, Oecologia, 91, 350–359, 1992.

Kosugi, Y., Takanashi, S., Tanaka, H., Ohkubo, S., Tani, M., Yano, M., and Katayama, T.: Evapotranspiration over a Japanese cypress forest. I. Eddy covariance fluxes and surface conductance characteristics for 3years, Journal of Hydrology, 337, 269–283, 2007.

Kowalczyk, E. A., Wang, Y. P., Wang, P., Law, R. H., and Davies, H. L.: The CSIRO Atmosphere Biosphere Land Exchange (CABLE) model for use in climate models and as an offline model, Tech. Rep. CSIRO Marine and Atmospheric Research paper 013, CSIRO, CABLE model, 2006.

Kumagai, T., Saitoh, T. M., Sato, Y., Morooka, T., Manfroi, O. J., Kuraji, K., and Suzuki, M.: Transpiration, canopy conductance and the decoupling coefficient of a lowland mixed dipterocarp forest in Sarawak, Borneo: dry spell effects, Journal of Hydrology, 287, 237–251, 2004.

Launiainen, S.: Seasonal and inter-annual variability of energy exchange above a boreal Scots pine forest, Biogeosciences, 7, 3921–3940, 2010.

Law, B., Falge, E., Gu, L. v., Baldocchi, D., Bakwin, P., Berbigier, P., Davis, K., Dolman, A., Falk, M., Fuentes, J., et al.: Environmental controls over carbon dioxide and water vapor exchange of terrestrial vegetation, Agricultural and Forest Meteorology, 113, 97–120, 2002.

Lee, X. and Black, T. A.: Atmospheric turbulence within and above a Douglas-fir stand. Part II: Eddy fluxes of sensible heat and water vapour, Boundary-Layer Meteorology, 64, 369–389, 1993.

Lin, Y.-S., Medlyn, B. E., Duursma, R. A., Prentice, I. C., Wang, H., Baig, S., Eamus, D., de Dios, V. R., Mitchell, P., Ellsworth, D. S., de Beeck, M. O., Wallin, G., Uddling, J., Tarvainen, L., Linderson, M.-L., Cernusak, L. A., Nippert, J. B., Ocheltree, T. W., Tissue, D. T., Martin-StPaul, N. K., Rogers, A., Warren, J. M., De Angelis, P., Hikosaka, K., Han, Q., Onoda, Y., Gimeno, T. E., Barton, C. V. M., Bennie, J., Bonal, D., Bosc, A., Low, M., Macinins-Ng, C., Rey, A., Rowland, L., Setterfield, S. A., Tausz-Posch, S., Zaragoza-Castells, J., Broadmeadow, M. S. J., Drake, J. E., Freeman, M., Ghannoum, O., Hutley, L. B., Kelly, J. W., Kikuzawa, K., Kolari, P., Koyama, K., Limousin, J.-M., Meir, P., Lola da Costa, A. C., Mikkelsen, T. N., Salinas, N., Sun, W., and Wingate, L.: Optimal stomatal behaviour around the world, Nature Climate Change, 5, 459–464, 2015.

Lindroth, A.: Aerodynamic and canopy resistance of short-rotation forest in relation to leaf area index and climate, Boundary-Layer Meteorology, 66, 265–279, 1993.

Loustau, D., Berbigier, P., Roumagnac, P., Arruda-Pacheco, C., David, J., Ferreira, M., Pereira, J., and Tavares, R.: Transpiration of a 64-year-old maritime pine stand in Portugal, Oecologia, 107, 33–42, 1996.

Magnani, F., Leonardi, S., Tognetti, R., Grace, J., and Borghetti, M.: Modelling the surface conductance of a broad-leaf canopy: effects of partial decoupling from the atmosphere, Plant, Cell & Environment, 21, 867–879, 1998.

Mahmood, K., Morris, J., Collopy, J., and Slavich, P.: Groundwater uptake and sustainability of farm plantations on saline sites in Punjab province, Pakistan, Agricultural Water Management, 48, 1–20, 2001.

Martin, P.: The significance of radiative coupling between vegetation and the atmosphere, Agricultural and Forest Meteorology, 49, 45–53, 1989.

Martin, T., Brown, K., Kučera, J., Meinzer, F., Sprugel, D., and Hinckley, T.: Control of transpiration in a 220-year-old Abies amabilis forest, Forest Ecology and Management, 152, 211–224, 2001.

McElwain, J. C. and Chaloner, W. G.: Stomatal density and index of fossil plants track atmospheric carbon dioxide in the Palaeozoic, Annals of Botany, 76, 389–395, 1995.

McNaughton, K. and Jarvis, P.: Water Deficits and Plant Growth, vol. 7, chap. Predicting effects of vegetation changes on transpiration and evaporation, pp. 1–47, Academic Press, New York, 1983a.

McNaughton, K. and Jarvis, P.: Water Deficits and Plant Growth, Vol. VII, chap. Predicting effects of vegetation changes on transpiration and evaporation, pp. 1–47, Academic Press, San Diego, 1983b.

McNaughton, K. and Jarvis, P.: Effects of spatial scale on stomatal control of transpiration, Agricultural and Forest Meteorology, 54, 279–302, 1991.

Medlyn, B., Barton, C., Broadmeadow, M., Ceulemans, R., De Angelis, P., Forstreuter, M., Freeman, M., Jackson, S., Kellomaki, S., Laitat, E., Rey, A., Roberntz, P., Sigurdsson, B., Strassemeyer, J., Wang, K., Curtis, P., and Jarvis, P.: Stomatal conductance of forest species after long-term exposure to elevated CO_2 concentration: a synthesis, New Phytologist, 149, 247–264, 2001.

Medlyn, B. E., De Kauwe, M. G., Lin, Y.-S., Knauer, J., Duursma, R. A., Williams, C. A., Arneth, A., Clement, R., Isaac, P., Limousin, J.-M., Linderson, M.-L., Meir, P., Martin-StPaul, N., and Wingate, L.: How do leaf and ecosystem measures of water-use efficiency compare?, New Phytologist, 2017.

Meinzer, F., Goldstein, G., Holbrook, N., Jackson, P., and Cavelier, J.: Stomatal and environmental control of transpiration in a lowland tropical forest tree, Plant, Cell &, Environment, 16, 429–436, 1993.

Meinzer, F., Andrade, J., Goldstein, G., Holbrook, N., Cavelier, J., and Jackson, P.: Control of transpiration from the upper canopy of a tropical forest: the role of stomatal, boundary layer and hydraulic architecture components, Plant, Cell & Environment, 20, 1242–1252, 1997.

Meirelles, M., Franco, A., Farias, S., and Bracho, R.: Evapotranspiration and plant–atmospheric coupling in a Brachiaria brizantha pasture in the Brazilian savannah region, Grass and Forage Science, 66, 206–213, 2011.

Mielke, M. S., Oliva, M., de Barros, N. F., Penchel, R. M., Martinez, C. A., and de Almeida, A. C.: Stomatal control of transpiration in the canopy of a clonal Eucalyptus grandis plantation, Trees-Structure and Function, 13, 152–160, 1999.

Miner, G. L., Bauerle, W. L., and Baldocchi, D. D.: Estimating the sensitivity of stomatal conductance to photosynthesis: A review, Plant, Cell & Environment, 2017.

Morison, J. I. L.: Sensitivity of stomata and water use efficiency to high CO_2, Plant, Cell &, Environment, 8, 467–474, 1985.

Motzer, T., Munz, N., Küppers, M., Schmitt, D., and Anhuf, D.: Stomatal conductance, transpiration and sap flow of tropical montane rain forest trees in the southern Ecuadorian Andes, Tree Physiology, 25, 1283–1293, 2005.

Nicolás, E., Barradas, V., Ortuño, M., Navarro, A., Torrecillas, A., and Alarcón, J.: Environmental and stomatal control of transpiration, canopy conductance and decoupling coefficient in young lemon trees under shading net, Environmental and Experimental Botany, 63, 200–206, 2008.

Oleson, K. W., Lawrence, D. M., Bonan, G. B., Drewniak, B., Huang, M., Koven, C. D., Levis, S., Li, F., Riley, W. J., Subin, Z. M., Swenson, S. C., Thornton, P. E., Bozbiyik, A., Fisher, R., Heald, C. L., Kluzek, E., Lamarque, J.-F., Lawrence, P. J., Leung, L. R., Lipscomb, W., Muszala, S., Ricciuto, D. M., Sacks, W., Sun, Y., Tang, J., and Yang, Z.-L.: Technical Description of version 4.5 of the Community Land Model (CLM), NCAR Technical Note NCAR/TN-503+STR, National Center for Atmospheric Research. Climate and Global Dynamics Division, National Center for Atmospheric Research, P.O. Box 3000, Boulder, Colarado, 2013.

Raupach, M. and Finnigan, J.: 'Single-layer models of evaporation from plant canopies are incorrect but useful, whereas multilayer models are correct but useless': Discuss, Functional Plant Biology, 15, 705–716, 1988.

Raupach, M., Finkele, K., and Zhang, L.: SCAM (Soil-Canopy-Atmosphere Model): Description and comparison with field data, Aspendale, Australia: CSIRO CEM Technical Report, p. 81, 1997.

San José, J. J., Montes, R. A., and Florentino, A.: Water flux through a semi-deciduous forest grove of the Orinoco savannas, Oecologia, 101, 141–150, 1995.

Sánchez, J., Caselles, V., and Rubio, E.: Analysis of the energy balance closure over a FLUXNET boreal forest in Finland, Hydrology and Earth System Sciences, 14, 1487–1497, 2010.

Sitch, S., Smith, B., Prentice, I. C., Arneth, A., Bondeau, A., Cramer, W., Kaplan, J., Levis, S., Lucht, W., Sykes, M., Thonicke, K., and Venevski, S.: Evaluation of ecosystem dynamics, plant geography and terrestrial carbon cycling in the LPJ Dynamic Vegetation Model, Global Change Biology, 9, 161–185, 2003.

Smith, D., Jarvis, P., and Odongo, J.: Management of windbreaks in the Sahel: the strategic implications of tree water use, Agroforestry systems, 40, 83–96, 1998.

Steduto, P. and Hsiao, T. C.: Maize canopies under two soil water regimes: III. Variation in coupling with the atmosphere and the role of leaf area index, Agricultural and Forest Meteorology, 89, 201–213, 1998.

Stoy, P., Katul, G., SIQUEIRA, M., JUANG, J., Novick, K., McCARTHY, H., Christopher Oishi, A., Uebelherr, J., KIM, H., and Oren, R.: Separating the effects of climate and vegetation on evapotranspiration along a successional chronosequence in the southeastern US, Global Change Biology, 12, 2115–2135, 2006.

Su, Z., Schmugge, T., Kustas, W., and Massman, W.: An evaluation of two models for estimation of the roughness height for heat transfer between the land surface and the atmosphere, Journal of Applied Meteorology, 40, 1933–1951, 2001.

Takagi, K., Kimura, R., and Şaylan, L.: Variability of surface characteristics and energy flux patterns of sunn hemp (Crotalaria juncea L.) under well-watered conditions, Theoretical and applied climatology, 96, 261–273, 2009.

Tateishi, M., Kumagai, T., Suyama, Y., and Hiura, T.: Differences in transpiration characteristics of Japanese beech trees, Fagus crenata, in Japan, Tree physiology, 30, 748–760, 2010.

Thom, A. S.: Vegetation and the Atmosphere, chap. Momentum, Mass and Heat Exchange of Plant Communities, pp. 57–109, Academic Press, London, 1975.

Wever, L. A., Flanagan, L. B., and Carlson, P. J.: Seasonal and interannual variation in evapotranspiration, energy balance and surface conductance in a northern temperate grassland, Agricultural and Forest meteorology, 112, 31–49, 2002.

White, D., Beadle, C., and Worledge, D.: Control of transpiration in an irrigated Eucalyptus globulus Labill. plantation, Plant, Cell & Environment, 23, 123–134, 2000.

Whitehead, D., Jarvis, P. G., and Waring, R. H.: Stomatal conductance, transpiration, and resistance to water uptake in a Pinus sylvestris spacing experiment, Canadian Journal of Forest Research, 14, 692–700, 1984.

Williams, C. A., Reichstein, M., Buchmann, N., Baldocchi, D., Beer, C., Schwalm, C., Wohlfahrt, G., Hasler, N., Bernhofer, C., Foken, T., et al.: Climate and vegetation controls on the surface water balance: Synthesis of evapotranspiration measured across a global network of flux towers, Water Resources Research, 48, 2012.

Wilson, K., Goldstein, A., Falge, E., Aubinet, M., Baldocchi, D., Berbigier, P., Bernhofer, C., Ceulemans, R., Dolman, H., Field, C., et al.: Energy balance closure at FLUXNET sites, Agricultural and Forest Meteorology, 113, 223–243, 2002.

Wilson, K. B. and Baldocchi, D. D.: Seasonal and interannual variability of energy fluxes over a broadleaved temperate deciduous forest in North America, Agricultural and Forest Meteorology, 100, 1–18, 2000.

Wohlfahrt, G., Haslwanter, A., Hörtnagl, L., Jasoni, R. L., Fenstermaker, L. F., Arnone, J. A., and Hammerle, A.: On the consequences of the energy imbalance for calculating surface conductance to water vapour, Agricultural and forest meteorology, 149, 1556–1559, 2009.

Woodward, F. and Kelly, C.: The influence of CO_2 concentration on stomatal density, New Phytologist, 131, 311–327, 1995.

Woodward, F. I., Smith, T. M., and Emanuel, W. R.: A global land primary productivity and phytogeography model, Global Biogeochemical Cycles, 9, 471–490, 1995.

Wullschleger, S. D., Meinzer, F., and Vertessy, R.: A review of whole-plant water use studies in tree, Tree physiology, 18, 499–512, 1998.

Wullschleger, S. D., Wilson, K. B., and Hanson, P. J.: Environmental control of whole-plant transpiration, canopy conductance and estimates of the decoupling coefficient for large red maple trees, Agricultural and Forest Meteorology, 104, 157–168, 2000.

Zeppel, M. and Eamus, D.: Coordination of leaf area, sapwood area and canopy conductance leads to species convergence of tree water use in a remnant evergreen woodland, Australian Journal of Botany, 56, 97–108, 2008.

5 Zhang, Z. Z., Zhao, P., McCarthy, H. R., Zhao, X. H., Niu, J. F., Zhu, L. W., Ni, G. Y., Ouyang, L., and Huang, Y. Q.: Influence of the decoupling degree on the estimation of canopy stomatal conductance for two broadleaf tree species, Agricultural and Forest Meteorology, 221, 230–241, 2016.

Zhou, L., Zhou, G., Liu, S., and Sui, X.: Seasonal contribution and interannual variation of evapotranspiration over a reed marsh (Phragmites australis) in Northeast China from 3-year eddy covariance data, Hydrological processes, 24, 1039–1047, 2010.

10 Zhu, P., Zhuang, Q., Ciais, P., Welp, L., Li, W., and Xin, Q.: Elevated atmospheric CO2 negatively impacts photosynthesis through radiative forcing and physiology-mediated climate feedback, Geophysical Research Letters, 2017.

Table 1: Literature summary of decoupling coefficients, see Table A2 for summaries of individual studies. Plant functional types (PFT) are defined as: ENF - evergreen needle leaved forest, EBF - evergreen broadleaved forest, DBF - deciduous broadleaved forest, TRF - tropical rain forest, SAV - savanna, SHB - shrub, GRA - grasses, C3C - C_3 crops, C4C - C_4 crops.

PFT	Mean	Standard Deviation	Min	Max	Number of studies
ENF	0.19	0.1	0.06	0.43	13
EBF	0.26	0.13	0.1	0.63	12
DBF	0.36	0.18	0.1	0.7	11
TRF	0.57	0.28	0.25	0.9	11
SAV	0.14	—	—	—	1
SHB	0.27	0.19	0.13	0.4	2
GRA	0.33	0.1	0.21	0.45	4
C3C	0.4	0.28	0.2	0.59	2
C4C	0.58	—	—	—	1
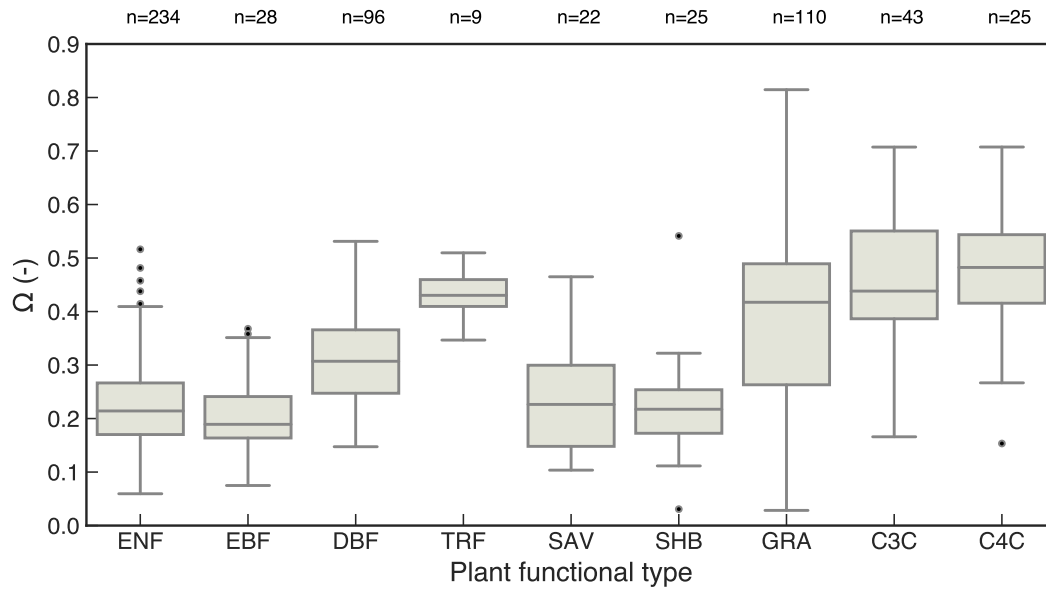
Figure 1. Box and whisker plot (line, median; box, inter-quartile range) showing the estimated coupling coefficient (Ω) from FLUXNET data, grouped by plant functional type. Whiskers extend to 1.5 times the inter-quartile range, with dots outside of the whiskers showing outliers. Plant functional types are defined as: ENF - evergreen needle leaved forest, EBF - evergreen broadleaved forest, DBF - deciduous broadleaved forest, TRF - tropical rain forest, SAV - savanna, SHB - shrub, GRA - grasses, C3C - C_3 crops, C4C - C_4 crops. Values of n indicate the number of site-years for FLUXNET.
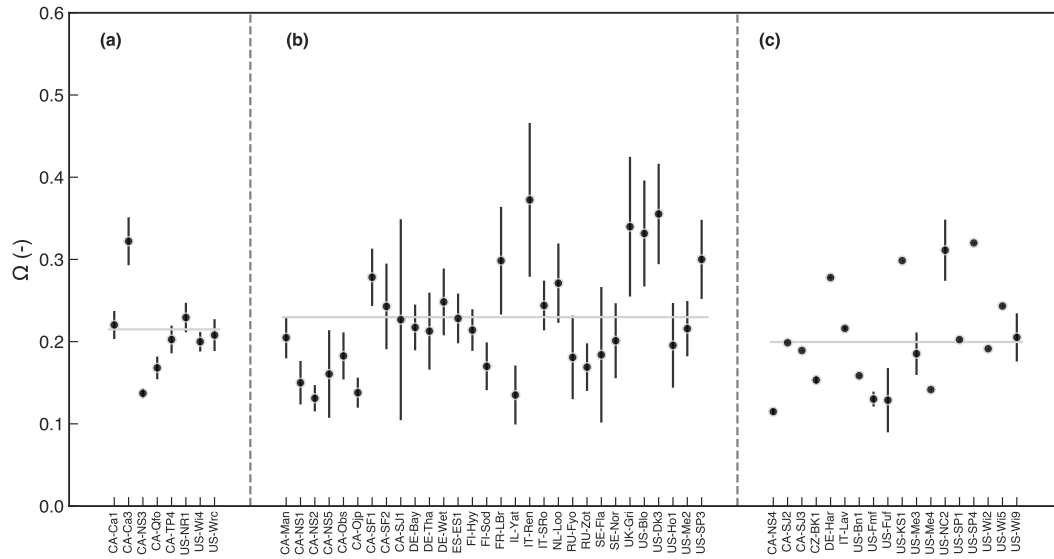
Figure 2. Values of the coupling coefficient (Ω) for sites from the evergreen needleleaf forests (ENF) plant functional type. Estimated values of Ω have been split into: (a) sites where the coefficient of variation (COV) is < 20%; (b) sites where the COV is > 20%; and (c) sites with only two years of data. Site errorbars represent one standard deviation (site year variation) in estimated Ω values. Solid horizontal grey lines show overall mean coupling coefficients.
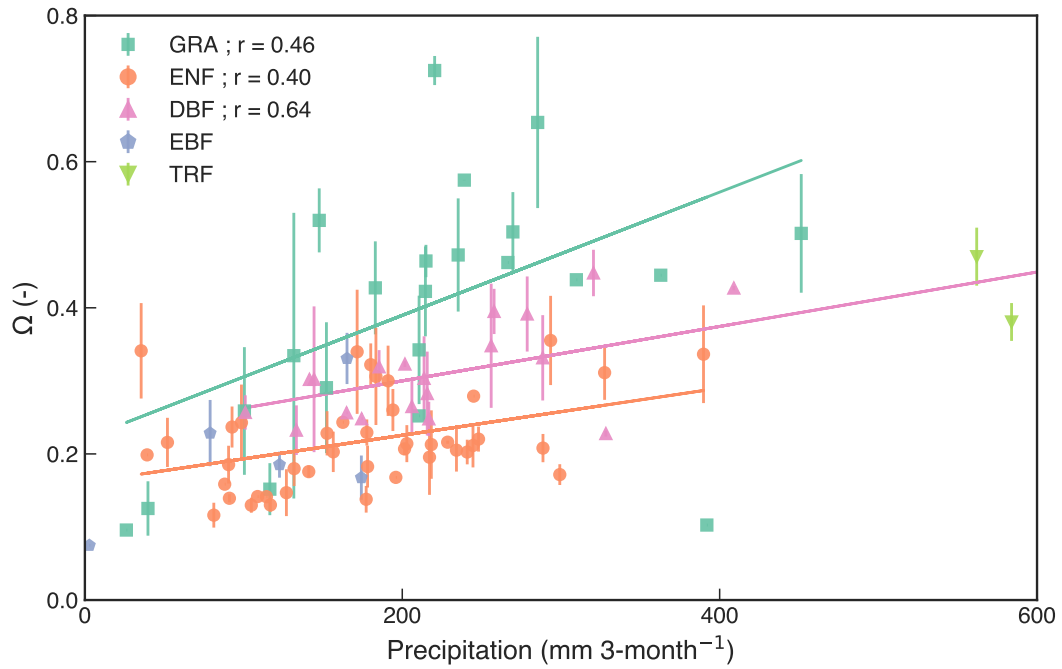
Figure 3. Values of the estimated coupling coefficient (Ω) for forest (ENF, EBF, DBF, TRF) vegetation and grasses as a function of precipitation in the three most productive months. Only data were 90% of the three most productive months were flagged as "good" are shown. Lines indicate statistically significant regressions (P < 0.05). Plant functional types are defined as: GRA - grasses, ENF - evergreen needle leaved forest, EBF - evergreen broadleaved forest, DBF - deciduous broadleaved forest and TRF - tropical rain forest.
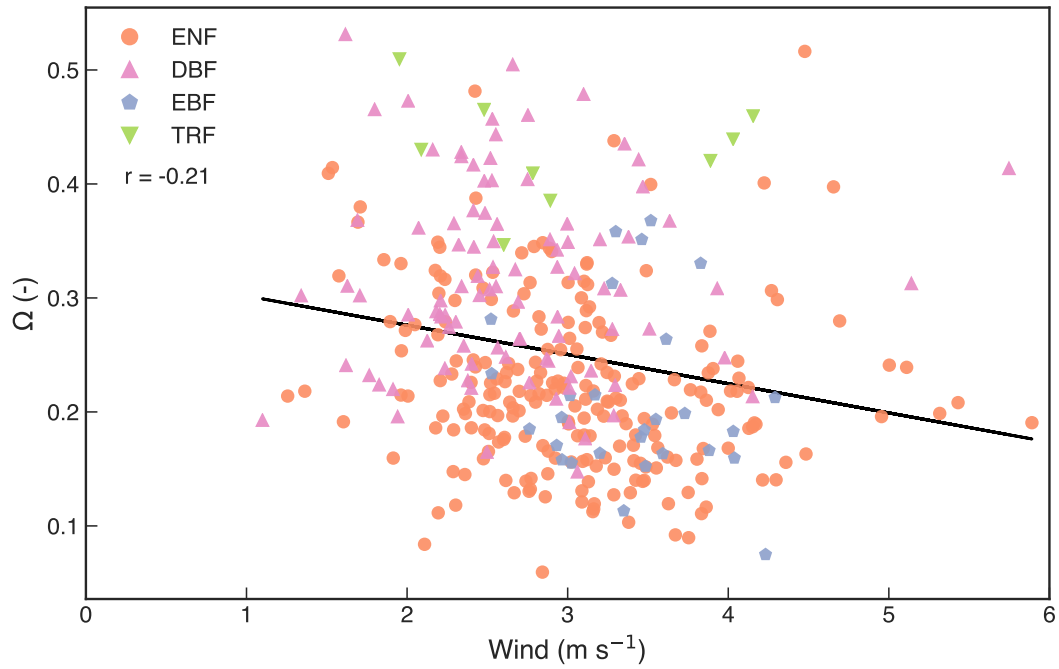
Figure 4. Values of the estimated coupling coefficient (Ω) for forest (ENF, EBF, DBF, TRF) vegetation as a function of wind speed. Line indicates statistically significant regression ($P < 0.05$), r is the correlation coefficient. Plant functional types are defined as: ENF - evergreen needle leaved forest, EBF - evergreen broadleaved forest, DBF - deciduous broadleaved forest, TRF - tropical rain forest.

Appendix A
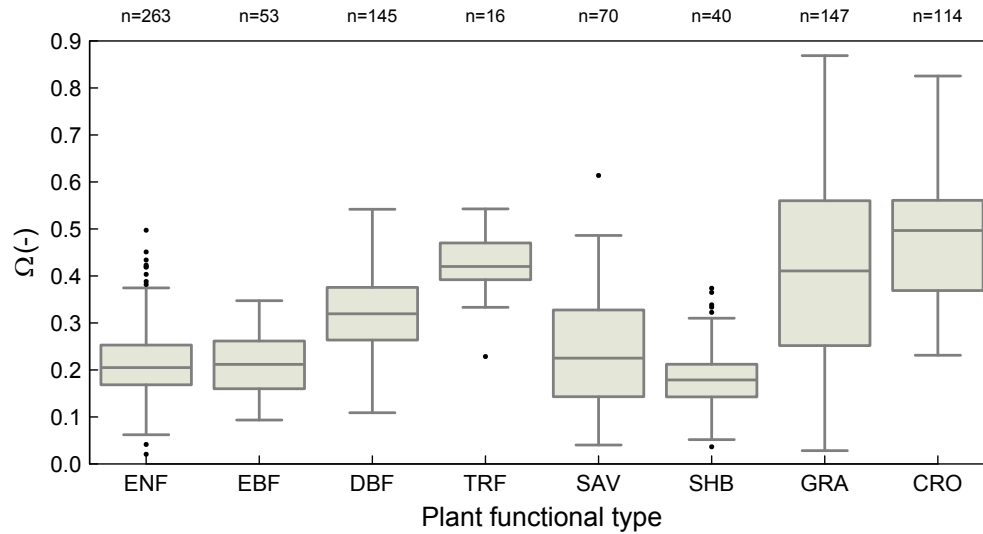
Figure A1. Box and whisker plot (line, median; box, inter-quartile range) showing the estimated coupling coefficient (Ω) from FLUXNET2015 data, grouped by plant functional type. Whiskers extend to 1.5 times the inter-quartile range, with dots outside of the whiskers showing outliers. Plant functional types are defined as: ENF - evergreen needle leaved forest, EBF - evergreen broadleaved forest, DBF - deciduous broadleaved forest, TRF - tropical rain forest, SAV - savanna, SHB - shrub, GRA - grasses, C3C - C_3 crops, C4C - C_4 crops. Values of n indicate the number of site-years for FLUXNET.
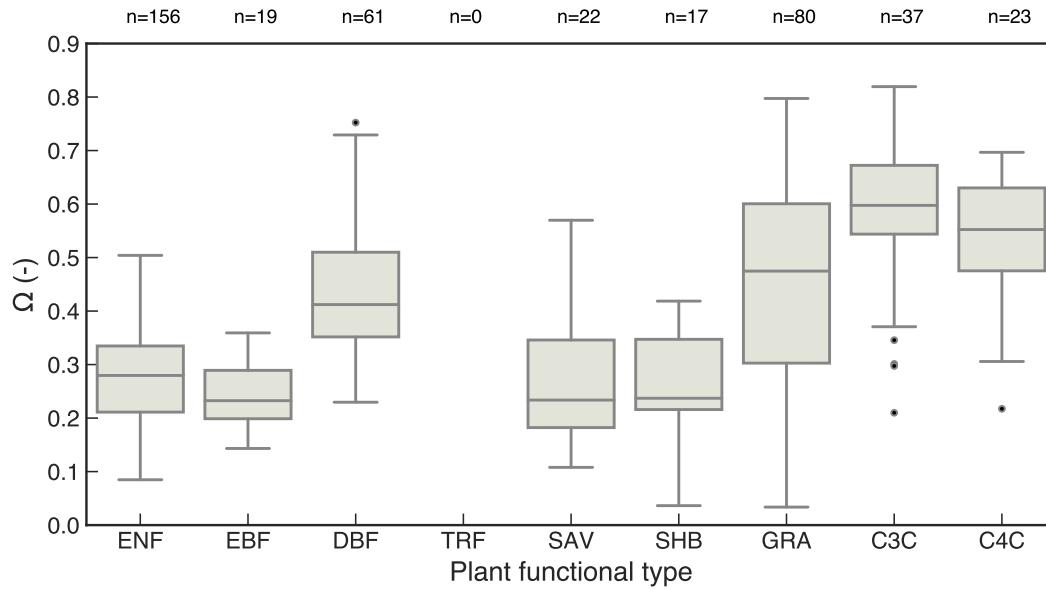
Figure A2. Box and whisker plot (line, median; box, inter-quartile range) showing the estimated coupling coefficient (Ω) from FLUXNET data, grouped by plant functional type. These data have been corrected for energy imbalance, adjusting the Bowen-ratio by the imbalance across the three most productive months. Whiskers extend to 1.5 times the inter-quartile range, with dots outside of the whiskers showing outliers. Plant functional types are defined as: ENF - evergreen needle leaved forest, EBF - evergreen broadleaved forest, DBF - deciduous broadleaved forest, TRF - tropical rain forest, SAV - savanna, SHB - shrub, GRA - grasses, C3C - C_3 crops, C4C - C_4 crops. Values of n indicate the number of site-years for FLUXNET.

Table A1: FLUXNET site years used in analysis.

Site ID	Years
AT-Neu	2002 2003 2004 2005
AU-How	2001 2002 2003 2004 2006
AU-Tum	2001 2002 2003 2004 2005 2006
AU-Wac	2005 2006 2007
BE-Lon	2004 2005 2006
BW-Ghg	2003
BW-Ghm	2003
BW-Ma1	1999 2000 2001
CA-Ca1	1998 1999 2000 2001 2002 2003 2004 2005
CA-Ca3	2001 2002 2003 2004 2005
CA-Let	1998 1999 2000 2001 2002 2003 2004 2005
CA-Man	1994 1995 1997 1998 1999 2000 2001 2002 2003
CA-NS1	2002 2003 2004
CA-NS2	2002 2003 2004 2005
CA-NS3	2001 2002 2004 2005
CA-NS4	2003 2004
CA-NS5	2001 2002 2003 2004 2005
CA-NS6	2001 2002 2003 2004 2005
CA-Oas	1997 1999 2000 2001 2002 2003 2004 2005
CA-Obs	1999 2000 2001 2002 2003 2004 2005
CA-Ojp	1999 2000 2001 2002 2003 2004 2005
CA-Qfo	2003 2004 2005 2006
CA-SF1	2003 2004 2005
CA-SF2	2003 2004 2005
CA-SJ1	2003 2004 2005
CA-SJ2	2005
CA-SJ3	2005
CA-TP4	2003 2004 2005
CG-Tch	2006
CH-Oe1	2003 2004 2005
CN-Du1	2005 2006
CN-Du2	2006

Table A1 continued from previous page

Site ID	Years
CN-HaM	2002 2003
CN-Xi1	2006
CN-Xi2	2006
CZ-BK1	2004 2005
CZ-BK2	2004
DE-Bay	1996 1997 1998 1999
DE-Geb	2004 2005 2006
DE-Gri	2005 2006
DE-Hai	2000 2001 2002 2003 2004 2005 2006
DE-Har	2005 2006
DE-Kli	2004 2005 2006
DE-Meh	2003 2004 2005 2006
DE-Tha	1996 1997 1998 1999 2000 2001 2002 2003 2004 2005
DE-Wet	2002 2003 2004 2005 2006
DK-Fou	2005
DK-Lva	2005
DK-Ris	2004
DK-Sor	2004 2005
ES-ES1	2000 2002 2003 2004 2005 2006
ES-ES2	2004 2005 2006
ES-LMa	2004 2005 2006
ES-VDA	2004 2005 2006
FI-Hyy	1998 1999 2000 2001 2002 2003 2004 2006
FI-Sod	2002 2003 2004 2005 2006
FR-Aur	2005
FR-Fon	2005 2006
FR-Gri	2005 2006
FR-Hes	1997 1998 1999 2000 2001 2002 2003 2004 2005 2006
FR-LBr	1996 1997 1998 2000 2003 2004 2005 2006
FR-Lam	2005
FR-Lq1	2005
FR-Lq2	2004 2005

Site ID	Years
FR-Pue	2000 2001 2002 2003 2004 2005 2006
GF-Guy	2004 2005 2006
HU-Bug	2002 2003 2004 2005 2006
HU-Mat	2004 2005 2006
ID-Pag	2002 2003
IE-Ca1	2004 2005 2006
IE-Dri	2004 2005
IL-Yat	2001 2002 2003 2006
IS-Gun	1996 1997 1998
IT-Amp	2002 2003 2004 2005 2006
IT-BCi	2005 2006
IT-Be2	2006
IT-Cas	2006
IT-Col	1998 1999 2004 2005 2006
IT-Cpz	1997 2000 2001 2002 2003 2004 2005 2006
IT-LMa	2004 2005 2006
IT-Lav	2004 2006
IT-MBo	2003 2004 2005 2006
IT-Mal	2004
IT-Noe	2004 2005 2006
IT-Non	2001 2002 2003 2006
IT-PT1	2003 2004
IT-Ren	2000 2001 2002 2003 2004
IT-Ro1	2000 2002 2003 2004 2005 2006
IT-Ro2	2004 2005 2006
IT-SRo	2000 2002 2003 2004 2005 2006
IT-Vig	2004
JP-Mas	2002 2003
NL-Ca1	2003 2004 2005 2006
NL-Hor	2006
NL-Lan	2005
NL-Loo	1996 1997 1998 1999 2001 2002 2003 2004 2006

Site ID	Years
PT-Esp	2002 2004 2006
PT-Mi1	2005
PT-Mi2	2004 2005 2006
RU-Cok	2005
RU-Fyo	1998 1999 2002 2003 2004 2005 2006
RU-Ha1	2003 2004
RU-Zot	2002 2003 2004
SE-Abi	2005
SE-Fla	1996 1997 1998 2001 2002
SE-Nor	1996 1997 1998 2005
UK-EBu	2004
UK-ESa	2004 2005
UK-Gri	1998 2000 2001 2006
UK-Ham	2004 2005
UK-Her	2006
UK-PL3	2005 2006
US-ARM	2003 2004 2005 2006
US-Aud	2002 2003 2004 2005 2006
US-Bar	2004 2005
US-Bkg	2004 2005 2006
US-Blo	1997 1998 1999 2000 2001 2002 2003 2004 2005
US-Bn1	2003
US-Bn2	2003
US-Bo1	1996 1997 1998 1999 2000 2001 2002 2003 2004 2005 2006 2007
US-Bo2	2004 2005 2006
US-CaV	2004 2005
US-Dk1	2001 2002 2003 2004 2005
US-Dk2	2003 2004
US-Dk3	2001 2002 2003 2004 2005
US-FPe	2000 2001 2002 2003 2004 2005 2006
US-Fmf	2005 2006
US-Fuf	2005 2006

Table A1 continued from previous page

Site ID	Years
US-Fwf	2005 2006
US-Goo	2002 2003 2004 2005 2006
US-Ha1	1992 1993 1994 1995 1996 1997 1998 1999 2000 2001 2003 2005 2006
US-Ho1	1996 1997 1998 1999 2000 2001 2002 2003
US-IB1	2005 2006 2007
US-IB2	2004 2006 2007
US-KS1	2002
US-KS2	2002 2003 2004 2005 2006
US-MMS	2000 2001 2002
US-MOz	2004 2005 2006
US-Me2	2003 2004 2005
US-Me3	2004 2005
US-Me4	2000
US-NC2	2005 2006
US-NR1	1999 2000 2002 2003
US-Ne1	2001 2002 2003 2004 2005
US-Ne2	2001 2002 2003 2004 2005
US-Ne3	2001 2002 2003 2004
US-SO2	1997 1998 1999 2004 2005 2006
US-SO3	1997 1998 2005 2006
US-SP1	2005
US-SP3	1999 2000 2001 2002 2003 2004
US-SP4	1998
US-SRM	2004 2005 2006
US-Ton	2001 2002 2003 2004 2005 2006
US-UMB	1999 2000 2001 2002 2003
US-Var	2001 2002 2003 2004 2005 2006
US-WCr	1999 2000 2001 2002 2003 2004 2005 2006
US-Wi1	2003
US-Wi2	2003
US-Wi4	2003 2004 2005
US-Wi5	2004

Table A1 continued from previous page

Site ID	Years
US-Wi9	2004 2005
US-Wkg	2004 2005 2006
US-Wrc	1998 1999 2000 2001 2002 2004 2005 2006
VU-Coc	2001 2002 2003 2004

Table A2: Literature summary of decoupling coefficients. Where possible we have summarised data from the growing season during daylight hours. Plant functional types (PFT) are defined as: ENF - evergreen needle leaved forest, EBF - evergreen broadleaved forest, DBF - deciduous broadleaved forest, TRF - tropical rain forest, SAV - savanna, SHB - shrub, GRA - grasses, C3C - C_3 crops, C4C - C_4 crops. Where E is transpiration, u_* is the frictional velocity, EC is eddy covariance, PM is Penman-Monteith, R_{tot} is the total resistance, R_a is the aerodynamic resistance, PAR is Photosynthetically Active Radiation and TC is the total conductance. The simple gradient approach refers to an estimation of G_s from vapour pressure deficit, pressure, and transpiration. Method refers to the approach to estimating Ω: (1) - default, as in this manuscript (amphistomatous vegetation); (2) hypostomatous vegetation; and (3) accounting for radiative coupling following Martin (1989).

PFT	Dominant species	Ω	Scale	Method	G_a	G_b	G_s	Reference
ENF	*Abies amabilis*	0.18	Stand	2	f(wind, roughness, radiation)	f(wind)	Inverted PM with sap flow	Martin et al. (2001)
ENF	*Callitris glaucophylla* J.Thompson	0.15	Canopy	1	f(wind, roughness)	—	Inverted PM, *E* from sap flow	Zeppel and Eamus (2008)
ENF	*Chamaecyparis obtusa*	0.21	Canopy	1	f(wind, u_*)	—	Inverted PM, *E* from EC	Kosugi et al. (2007)
ENF	*Picea glauca*	0.4	Stand	1	f(wind, u_*)	—	Simplified PM with sap flow	Bladon et al. (2006)
ENF	*Picea abies*	0.19	Canopy	1	Inversion bulk transfer of sensible heat (EC)	—	Inversion bulk transfer of sensible and latent heat (EC)	Goldberg and Bernhofer (2008)
ENF	*Picea crassifolia*	0.06	Canopy	1	f(wind, u_*)	—	Inverted PM, *E* from EC	Gaofeng et al. (2014)
ENF	*Pinus elliotti*	0.43	Canopy	1	f(wind, roughness)	f(u_*)	Inverted PM, *E* from EC	Bracho et al. (2008)
ENF	*Pinus pinaster*	0.08	Stand	1	Empirical reln. between G_a & wind	—	Inverted PM, *E* from sap flow	Loustau et al. (1996)

PFT	Dominant species	Ω	Scale	Method	G_a	G_b	G_s	Reference
ENF	*Pinus sylvestris*	0.1	Stand	1	f(wind, height)	—	Leaf gas exchange	Whitehead et al. (1984)
ENF	*Pinus sylvestris*	0.32	Canopy	1	f(wind, u_*)	—	Inverted PM, *E* from EC	Launiainen (2010)
ENF	*Pinus taeda*	0.25	Canopy	1	f(roughness, u_*)	f(characteristic leaf dimension, wind)	Bottom-up model: f(VPD, LAI & radiation)	Stoy et al. (2006)
ENF	*Pseudotsuga menziesii*	0.26	Canopy	1	f(wind, u_*)	—	Inverted PM, *E* from EC	Jassal et al. (2009)
ENF	*Pseudotsuga menziesii*	0.15	Canopy	1	f(wind, u_*)	—	Inverted PM, *E* from EC	Lee and Black (1993)
EBF	*Acacia ampliceps*	0.28	Stand	3	Empirical relationship between G_a & wind speed	—	Inverted (simplified) PM, *E* from sap flow	Mahmood et al. (2001)
EBF	*Azadirachta indica*	0.28	Tree	2	f(leaf temperature)	—	Inverted (Simplified) PM from sap flow	Smith et al. (1998)
EBF	*Citrus limon*	0.12	Stand	1	f(wind, u_*)	—	$R_{tot} - R_a$, R_{tot} from simplified PM, E from sap flow	Nicolás et al. (2008)
EBF	*Eucalyptus camaldulensis*	0.33	Stand	3	Empirical relationship between G_a & wind speed	—	Inverted (simplified) PM, *E* from sap flow	Mahmood et al. (2001)

PFT	Dominant species	Ω	Scale	Method	G_a	G_b	G_s	Reference
EBF	*Eucalyptus crebra* F.Muell.	0.19	Canopy	1	f(wind, roughness)	—	Inverted PM, *E* from sap flow	Zeppel and Eamus (2008)
EBF	*Eucalyptus globulus*	0.63	Stand	1	TC – G_s	—	Simple gradient approach, *E* from sap flow	White et al. (2000)
EBF	*Eucalyptus grandis*	0.28	Stand	1	f(wind, u_*)	—	$R_{tot} - R_a$, R_{tot} from simplified PM, E from sap flow	Mielke et al. (1999)
EBF	*Eucalyptus urophylla*	0.1	Stand	1	f(wind, roughness)	—	Inverted PM, *E* from sap flow	Zhang et al. (2016)
EBF	*Nothofagus fusca*	0.24	Stand	1	f(wind, roughness)	—	Stomatal conductance from gas exchange upscaled by leaf area	Köstner et al. (1992)
EBF	*Quercus*	0.3	Canopy	1	f(roughness, u_*)	f(characteristic leaf dimension, wind)	Bottom-up model: f(VPD, LAI & PAR)	Stoy et al. (2006)
EBF	*Schima superba*	0.22	Stand	1	f(wind, roughness)	—	Inverted PM, *E* from sap flow	Zhang et al. (2016)

PFT	Dominant species	Ω	Scale	Method	G_a	G_b	G_s	Reference
EBF	*Vaccinium vitis-vidaea*	0.2	Canopy (under-storey only)	1	f(wind, u$_*$)	—	Inverted PM, *E* from EC	Iida et al. (2009)
DBF	*Acer rubrum*	0.23	Stand	1	f(wind, u$_*$)	f(u$_*$)	Inverted PM, *E* from sap flow	Wullschleger et al. (2000)
DBF	*Betula papyrifera*	0.36	Stand	1	f(wind, u$_*$)	—	Simplified PM from sap flow	Bladon et al. (2006)
DBF	*Fagus sylvatica*	0.28	Canopy	1	f(wind, roughness)	f(leaf size)	Bottom-up model: f(VPD, maximum G$_s$, temperature and radiation)	Magnani et al. (1998)
DBF	*Fagus crenata*	0.3	Stand	1	f(wind, roughness)	f(characteristic leaf dimension, wind)	Inverted PM, *E* from sap flow	Tateishi et al. (2010)
DBF	*Fagus sylvatica*	0.2	Canopy	1	f(wind, roughness)	—	Inverted PM, *E* from the Bowen ratio	Herbst (1995)
DBF	*Juglans regia*	0.37	Tree	2	—	f(leaf temperature, roughness)	Modelled following Jarvis (1976) and upscaled	Daudet et al. (1999)

PFT	Dominant species	Ω	Scale	Method	G_a	G_b	G_s	Reference
DBF	*Populus balsamifera*	0.4	Stand	1	f(wind, u_*)	—	Simplified PM with sap flow	Bladon et al. (2006)
DBF	*Populus trichocarpa x P. deltoides*	0.66	Canopy	3	TC – G_s	—	Simple gradient approach, *E* from sap flow	Hinckley et al. (1994)
DBF	*Quercus petraea*	0.1	Canopy	1	f(wind, roughness)	—	Inverted PM, *E* from EC	Granier and Bréda (1996)
DBF	*Salix viminalis*	0.7	Canopy	1	Inverted PM when the canopy is wet	—	Inverted PM, *E* from sap flow	Lindroth (1993)
DBF	—	0.41	Canopy	1	Surface layer similarity	f(u_*)	Inverted PM, *E* using the Bowen ratio (EC)	Wilson and Baldocchi (2000)
TRF	*Anacardium excelsum*	0.75	Tree	2	TC – G_s	—	Leaf gas exchange	Meinzer et al. (1993)
TRF	*Cecropia longipes*	0.9	Tree	2	TC – G_s & stomatal conductance	—	Leaf gas exchange	Meinzer et al. (1997)
TRF	*Ficus insipida*	0.82	Tree	2	TC — G_s	—	Leaf gas exchange	Meinzer et al. (1997)
TRF	*Hedyosmum anisodorum* Todzia	0.37	Leaf	1	—	f(wind, leaf extension)	Leaf gas exchange	Motzer et al. (2005)
TRF	*Luehea seemannii*	0.88	Tree	2	TC – G_s	—	Leaf gas exchange	Meinzer et al. (1997)
TRF	*Naucleopsis* sp.	0.27	Leaf	1	—	f(wind, leaf extension)	Leaf gas exchange	Motzer et al. (2005)

PFT	Dominant species	Ω	Scale	Method	G_a	G_b	G_s	Reference
TRF	*Psychotria brachiata* Ruiz & Pav.	0.27	Leaf	1	—	f(wind, leaf extension)	Leaf gas exchange	Motzer et al. (2005)
TRF	*Ruagea cf. pubescens* H. Karst.	0.25	Leaf	1	—	f(wind, leaf extension)	Leaf gas exchange	Motzer et al. (2005)
TRF	*Spondias mombin*	0.9	Tree	2	TC — G_s	—	Leaf gas exchange	Meinzer et al. (1997)
TRF	*Trichilia guianensis* Klotzsch	0.43	Leaf	1	—	f(wind, leaf extension)	Leaf gas exchange	Motzer et al. (2005)
TRF	—	0.43	Canopy	1	TC – G_a – f(wind, u_*)	—	Inverted PM, *E* from EC	Kumagai et al. (2004)
SAV	—	0.14	Stand	1	f(wind, roughness)	—	Inverted PM, *E* from EC	San José et al. (1995)
SHB	*Quer juliflora*	0.13	Stand	3	Empirical relationship between G_a & wind speed	—	Inverted (simplified) PM, *E* from sap flow	Mahmood et al. (2001)
SHB	*Quercus sp.*	0.4	Canopy	1	f(wind, roughness)	f(u_*)	Inverted PM, *E* from EC	Bracho et al. (2008)
GRA	*Brachiaria brizantha*	0.5	Canopy	1	f(wind, roughness)	f(u_*)	Inverted PM, *E* from EC	Meirelles et al. (2011)
ENF	*Festuca arundinaria* Shreb.	0.34	Canopy	1	f(roughness, u_*)	f(characteristic leaf dimension, wind)	Bottom-up model: f(VPD, LAI & radiation)	Stoy et al. (2006)
GRA	*Phragmites australis*	0.48	Canopy	1	f(wind, u_*)	f(u_*)	Inverted PM, *E* from EC	Zhou et al. (2010)

PFT	Dominant species	Ω	Scale	Method	G_a	G_b	G_s	Reference
GRA	—	0.45	Canopy	1	f(wind, u_*)	—	Inversion bulk transfer of sensible and latent heat (EC)	Goldberg and Bernhofer (2008)
GRA	—	0.49	Canopy	1	f(wind, u_*)	f(u_*)	Inverted PM, E from EC	Aires et al. (2008)
GRA	—	0.31	Canopy	1	f(wind, u_*)	f(u_*)	Inverted PM, E from EC	Hao et al. (2007)
GRA	—	0.21	Canopy	1	f(wind, u_*)	f(u_*)	Inverted PM, E from EC	Wever et al. (2002)
C3C	*Crotalaria juncea*	0.59	Canopy	1	f(wind, roughness)	—	Inverted PM, E from Bowen Ratio energy balance method	Takagi et al. (2009)
C3C	*Musa sp.*	0.2	Stand	1	f(wind, characteristic leaf dimension, LAI)	—	Inverted PM, E from sap flow Ratio energy balance method	Haijun et al. (2015)
C4C	*Zea mays*	0.58	Canopy	1	f(wind, roughness)	f(u_*)	Inverted PM, E from Bowen Ratio energy balance method	Steduto and Hsiao (1998)